SEMARAK ILMU PUBLISHING

Journal of Advanced Research in Micro and Nano Engineering

Journal homepage:
https://semarakilmu.com.my/journals/index.php/micro_nano_engineering/index
ISSN: 2756-8210

Influence of Accelerators and Filler Content on Physical Properties of Tin Dioxide Reinforced Deproteinized Natural Rubber Nanocomposites

Noraiham Mohamad[1], Jeefferie Abd Razak[1,*], Maizatul Aisyah Mohamad[1], Soh Tiak Chuan[2], Hairul Effendy Ab Maulod[2], Mohamad Iqbal Shueb[3], Qumrul Ahsan[4], Toibah Abd Rahim[1], Mohd Warikh Abd Rashid[1]

[1] Fakulti Teknologi dan Kejuruteraan Industri dan Pembuatan, Universiti Teknikal Malaysia Melaka, Hang Tuah Jaya, 76100 Durian Tunggal, Melaka, Malaysia
[2] Rubber Leisure Products Sdn. Bhd., Kawasan Perindustrian Serkam, 77300 Jasin, Melaka, Malaysia
[3] Radiation Processing Technology Division, Malaysian Nuclear Agency, Bangi, 43000 Kajang, Selangor, Malaysia
[4] University of Asia Pacific, 74/A, Green Road, Farmgate, Dhaka-1205, Bangladesh

ARTICLE INFO

Article history:
Received 27 July 2024
Received in revised form 3 September 2024
Accepted 19 October 2024
Available online 30 November 2024

Keywords:
Polymer matrix nanocomposites; natural rubber; tin dioxide; accelerator; physical properties; filler content

ABSTRACT

The global electrical industry is looking for sustainable materials in various domains, including electrical insulation cable materials. Tin dioxide (SnO_2) nanoparticles combined with deproteinized natural rubber (DPNR) have the potential to produce an excellent and green electrical insulation material that combines their parents' electrical properties. Yet, the processability is highly influenced by the curing system. The cure characteristics of rubber nanocomposites were investigated for the influence of different accelerators and SnO_2 content. The 2,20-dithiobis (benzothiazole) (MBTS)-cured compounds exhibit ultrafast curing and higher melt viscosity than the N-Cyclohexyl-2-benzothiazole sulphonamide (CBS)-cured nanocomposite compounds, regardless of the increment in SnO_2 loadings. Therefore, CBS-cured nanocomposites exhibit acceptable process safety, good processability and properties. The morphological, thermal and compositional analyses further supported the density, swelling behaviour and hardness of the DPNR nanocomposites of the selected accelerator system.

1. Introduction

Electrical insulation technology plays a pivotal role in cable systems. It entails the development of new insulation materials with improved dielectric strength, mechanical properties, environmental resilience and enhanced thermal conductivity by creating effective heat dissipation systems [1]. Natural rubber (NR)-based insulations for electrical wire date back to the electrical industry's infancy. Historically, producers discovered that adding various compounding components, such as mineral fillers, enhances rubber. Until the 1930s, natural rubber-based electrical insulation was the sole polymeric material utilized as a wire and cable dielectric [2]. Yet, there are reports on the weaknesses

* *Corresponding author.*
E-mail address: jeefferie@utem.edu.my

https://doi.org/10.37934/armne.26.1.3043

of NR insulation materials due to their less resistance to thermal degradation and ozone corresponding to their unsaturated backbone. Besides, it exhibits low oil and chemical resistance due to non-polarity [3]. Therefore, many researchers investigate various NR-based blends and composites with other elastomers such as NR-CR [4], NR-EDPM [5], thermoplastics example, NR-HDPE [5], biodegradable polymers such as NR-Chitosan [6] and NR-thermoplastic starch [7] and fillers for various purposes.

Filler materials, either microfibers, nanofibers or nanoparticles, have played an important role in altering the dielectric characteristics of NR-based materials. Some fillers were discovered to boost surface and volume resistivity, reducing leakage current and enhancing resistance to tracking and erosion [3]. These filler particles worked as a barrier against the flow of electrical charges. Various organic fibre and compounds (oil palm empty fruit bunch, potato starch nanocrystal) and inorganic fillers (alumina trihydrate, nano montmorillonite (MMT)) were found of increasing the surface and volume resistivity, capable of suppressing leakage current and improving resistance to tracking and erosion [3]. These nanoparticles acted as a barrier to the electrical charge movements. Meanwhile, there are nanofillers such as silicon dioxide, titanium dioxide and carbon nanomaterials that were reported to increase the partial discharge (PD) activities and decrease the electrical resistivity (iron oxide-carbon nanotubes and nickel-cobalt-zinc ferrite nanoparticles) [3,8]. Therefore, highly conductive filler materials such as carbon nanotubes are likely to have an undesirable impact on the dielectric properties of NR composites [8]. Hence, adding semiconductor nanofillers into the polymer matrix would be a promising solution for improving dielectric and mechanical properties.

Studies on incorporating SnO_2 nanoparticles into NR for electrical insulation and the effect of curing accelerators are limited. Hence, our studies served as a preliminary investigation into the possibility of SnO_2-reinforced DPNR nanocomposites as an electrically insulating material [9]. The environmentally friendly rutile structure SnO_2 is an n-type wide bandgap semiconductor with a bandgap of 3.6 eV [9]. Its nanocrystalline structure possesses remarkable electrical properties. Due to the high surface-to-volume ratio and quantum confinement effects, nanocrystalline. Nowadays, it offers tremendous advantages for various applications [10]. Tin oxide-based materials are used widely in various applications according to their inherent potential to be used as catalysts, photocatalysis, anode materials catalysis, electrocatalysis, optoelectronics, spintronics devices sensors, solar energy conversion, antistatic coatings, transparent conductive electrodes and electrochromic devices [10,11].

Calcination is a high-temperature process that can alter a material's physical and chemical properties. Numerous studies have shown that calcining nanofillers reduces their propensity to interact with water [12]. Zhuravlev *et al.,* [13] proposed that physically adsorbed water (dehydration), surface hydroxyl groups (surface dihydroxylation) and internal hydroxyl groups (internal dihydroxylation) of SiO_2 can be removed at temperatures ranging from 25 to 190 °C, 190 to 400 °C and 400 to 900 °C, respectively. At 900 °C, completely removing surface silanol and internal OH groups is possible, a reversible process when exposed to water later [13]. Despite the use of calcined nanofillers that can significantly enhance the dielectric properties of nanocomposites, as claimed by Rahim *et al.,* [12], this current study on SnO_2 nanoparticles is trying to investigate the loading effect of uncalcined fillers in the DPNR nanocomposites.

According to Mahyudin *et al.,* [14], polymer matrix composite properties are determined by the materials used and the interactions or bonding between the fibre and the matrix. In their work, filler content in polymer composites influenced the mechanical and biodegradability properties. Nevertheless, the chemical reaction between constituents results from rubber nanocomposites' mechanical properties and processability. It depends mostly on the types of filler and curing systems used [15]. Cure systems utilized in various natural rubber composites and nanocomposites can either

be conventional (CV), semi-efficient (Semi-EV) or efficient (EV). Crosslinks formed within the tightly packed molecular network during vulcanization and adding fillers and additives affect the properties of the rubber vulcanizates. The semi-EV is widely used due to its best processability and performance balance for product manufacturing and applications [16-18]. Ghorai *et al.,* [18] found that semi-EV showed the highest mechanical properties compared to CV and EV systems when optimizing the vulcanizing system in sulphur-crosslinked natural rubber (NR). Other research has proven that the type of accelerators also played a crucial role in affecting the cure characteristics and the mechanical properties of sulphur-cured rubber compounds [19]. While there have been limited studies on the incorporation of SnO_2 nanoparticles into NR for electrical insulation, our investigation into the effect of accelerators is crucial. Accelerators can influence the aging behaviour of insulating materials. A comprehensive study can reveal how accelerators affect material degradation over time, leading to insights into improving reliability and service life.

This research investigates the feasibility of producing DPNR/SnO_2 nanocomposites using melt compounding and semi-EV vulcanization. Two primary accelerator systems were compared using either CBS or MBTS for the vulcanization. The curing characteristics of 0.5, 1, 3 and 7 phr SnO_2 nanoparticles in a DPNR matrix were evaluated. The findings of the most suitable accelerator system are supported by hardness, density, swell measurement, SEM and FTIR analyses.

2. Methodology

The DPNR nanocomposite formulation used in the present study is given in Table 1. Deproteinized natural rubber, DPNR was supplied by the Malaysian Rubber Board.

Table 1
Formulations based on primary accelerator system

Ingredients (parts per hundred rubbers, phr)	Primary accelerator system	
	CBS	MBTS
DPNR	100	100
Zinc oxide	5	5
Stearic acid	2	2
Sulphur	1.5	1.5
N-Cyclohexyl-2-benzothiazole sulphonamide (CBS)	1.0	0
2,20-dithiobis (benzothiazole) (MBTS)	0	1.0
Tetramethylthiuram disulfide (TMTD)	0.3	0.3
N-(1,3-Dimethylbutyl)-N'-phenyl-p phenylenediamine (6PPD)	2.0	2.0
SnO_2 nanoparticles (phr)	0, 0.5, 1.0, 3.0 and 7.0	

Two compound systems using different curing accelerators were prepared using 100 phr of DPNR and uncalcined $_{SnO2}$ nanoparticle loadings at 0.5, 1, 3 and 7 phr through a melt compounding process. Curing additives: 1.5 phr of sulphur (S), 5 phr of zinc oxide (ZnO), 2 phr of stearic acid, 0.3 phr of tetramethyl thiuram disulphate (TMTD) and 2 phr of 6PPD. The formulation was designed based on the successful recipe of rubber nanocomposites by Mohamad *et al.,* [17]. The compounds were sulphur cured either by 1 phr MBTS or CBS accelerators. The DPNR nanocomposite compounds were prepared via the melt compounding method according to ASTM D-3182. The cure characteristics of the nanocomposites were assessed according to ASTM D2084. The test was performed using oscillating motorless rheometers. Samples of the respective compounds were tested at 150°C within 5 min of curing time. The maximum curing time (T_{90}), scorch time (T_{S2}), minimum torque (ML) and maximum torque (MH) were determined. Then, the torque difference (MH-ML) and cure rate index (CRI) were calculated. The formula for CRI is in Eq. (1) [20]:

$$CRI = {}^{100}/_{T_{90} - T_{S2}} \quad (1)$$

From the cure characteristics, the most suitable accelerator system was selected. The selected compounds were then compressed at 150°C and 150 kgf in a hot press.

Then, their properties were further characterized using several material testing and characterization techniques:

i. Density
ii. Hardness
iii. Swell measurement
iv. Compositional and morphological analyses.

The density test was conducted to measure the apparent density of the material using ASTM D792. Five specimens of each filler loading were tested and the average value was calculated. The swell measurement testing was determined from the relative weight of toluene absorption. The sample in the form of a rectangular sheet 10 mm long, 10 mm wide and 3.2 mm thick was weighed before and after being immersed in toluene. The sample was weighted after immersion for 24 hours to determine the wet weight. The calculation was performed utilizing the formula in Eq. (2), simplified of Kaliyathan *et al.,* [21]. The percentage increase in weight was calculated to the nearest 0.01 %. Ww is the wet weight and Wc is the conditional weight, refer to Eq. (2).

$$\text{Increase in weight, \%} = {}^{W_W - W_C}/_{W_C} \times 100 \quad (2)$$

Fourier Transform Infrared Spectroscopy (FTIR) analyses were performed on samples using an FTIR-6100typeA Spectrometer from JASCO. It was conducted to confirm the presence of functional groups and differences in the structure between pristine DPNR and DPNR/SnO_2 nanocomposites. This FTIR spectroscopy analysis was performed at the temperature of 25°C and was acquired in a resolution of 4.0 cm^{-1} at the wave number range of 400 cm^{-1} - 4000 cm^{-1} at a scanning speed of 2 mm s^{-1} with an aperture size of 7.1 mm. This analysis was performed using the attenuated total reflectance (ATR) technique.

The dynamic mechanical properties were evaluated using a DMTA IV from Rheometric Scientific. The samples, cut from a vulcanized slab, had dimensions of 5 mm x 50 mm and a thickness between 1.0 mm and 1.5 mm. The DMTA was set up with a sample gap of 20 mm, operating at a frequency of 10 Hz and a strain of 0.1%. The sample was initially cooled to -90°C and measurements were taken as it was heated at a rate of 20°C per minute.

Scanning electron microscopy (SEM) analysis was conducted on the tensile fractured surfaces using FESEM, Model Gemini SEM 500 from Carl Zeiss. The analysis was to examine the sample surface's morphology for the level of distribution, aggregation and failure modes. The examination was conducted at the voltage of 10kV using the secondary electron at the magnifications of 200X. Morphology and topology analyses were also performed using an Atomic Force Microscopy (AFM) provided by JPK Instruments. The samples were sectioned into smaller dimensions and positioned onto a glass slide. The measurement was conducted utilizing a contact mode cantilever.

3. Results and Discussion

3.1 Cure Characteristics

Figure 1 and Table 2 compare the effect of using either MBTS or CBS primary accelerators at different filler loadings on the cure characteristics of the DPNR/SnO_2 nanocomposites. The vulcanization characteristics of all rubber compounds were investigated by determining the torque-time relationship using the data. The cure characteristics are represented by the required time for 90% curing (T_{90}), the scorch time (T_{S2}), the maximum torque (MH), minimum torque (ML) and the torque difference (MH-ML) and the cure rate index (CRI).

It can be deduced from Figure 1 and Table 2 that incorporating SnO_2 nanoparticles has generally decreased the MH, ML and MH-ML in composites. The decrement in torque values has suggested that the filler particles might act as the plasticizers that soften the chain mobility under deformation. The MH can be regarded as a measure of the modulus of the composite [22]. The significantly decreased values in MH with filler loading are an indirect hint for improved flexibility of the composites and less stiffness under forces. Meanwhile, the ML is related to the viscosity of a compound. Incorporating SnO_2 nanoparticles moderately decreased the ML and thus lowered its viscosity under heat.

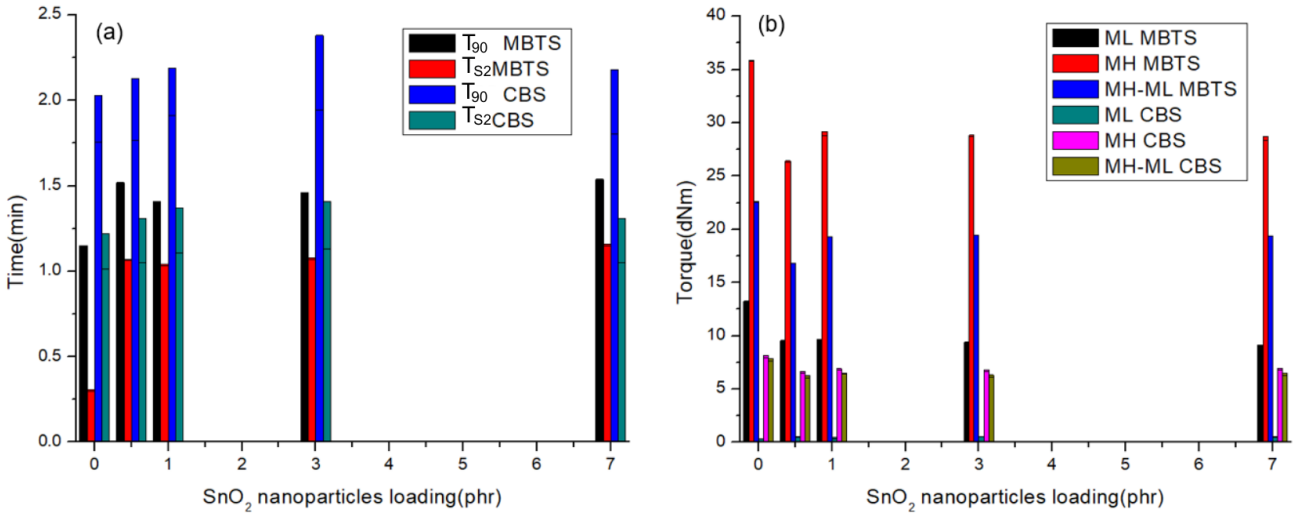

Fig. 1. Cure characteristics of SnO_2 nanoparticles reinforced DPNR nanocomposites

In most cases, the addition of fillers of a smaller size tends to impose extra resistance to flow due to higher restriction to the macromolecules' molecular motion, resulting in higher viscosity [22]. Similar patterns are seen for MH-ML values for both accelerator systems, which decrease with filler loadings. The MH-ML represents the dynamic shear modulus experienced by the material and it has an indirect relationship with the crosslink density of the composite. The presence of SnO_2 nanoparticles may reduce the number of efficient crosslinks required for the compound to cure. The finding is supported by the stability of the swelling percentage of the composites over 72 hours. It is evident that the swelling percentage was higher in the nanocomposites compared to the control sample. The DPNR nanocomposite formulation used in the present study is given in Table 1. Deproteinized natural rubber, DPNR was supplied by the Malaysian Rubber Board.

Table 2
Cure rate index (CRI) of SnO_2 nanoparticles reinforced DPNR nanocomposites

Cure Rate Index (CRI)	Filler loading (phr)					σ (±)
	0	0.5	1	3	7	
CBS system	135.00	138.96	142.86	151.51	156.25	16.44
MBTS system	120.48	227.27	263.46	263.16	256.41	3.35

In Figure 1(a), both T_{S2} and T_{90} were generally increased with SnO_2 loadings, especially when compared to the control samples (without SnO_2). The T_{S2} indicates how long a rubber compound can be worked at a given temperature before curing. Meanwhile, T_{90} represents the amount of time required for 90% curing. It is clear that the addition of filler significantly increased the T_{S2} and T_{90}, which represents delayed curing. The prolonged scorch with the addition of SnO_2 might result from higher surface activities between filler-matrix during the curing process. According to Nor and Othman [23], the long cure times demonstrated how adding filler particles could slow down the vulcanization of rubber composites. However, in this study, the highly specific surface areas of the SnO_2 nanoparticles and the charges on their surfaces are factors that facilitate the SnO_2 particles' ability to absorb the vulcanizing and curing chemicals. It agrees with the compositional analysis of the composites using FTIR analysis. The delay in the curing span of the rubber compound was due to a significant amount of bound water and hydroxyl groups on the surface of SnO_2. The FTIR analysis depicts various functional groups on the uncalcined SnO_2 particles. Similar results were reported by Chang *et al.,* [24] when the inclusion of organoclay in the mixture increased the cure time of EPDM-organo-montmorillonite hybrid nanocomposites. They suggested that the curing chemicals' absorption by the filler surface caused a prolonged cure time.

In comparison to the NR control sample, the CRI of the DPNR nanocomposites is significantly higher in all samples. As filler increased as shown in Table 2, the CRI value rose. It represents the ability of the SnO_2 nanoparticles to facilitate the curing process. This is because more SnO_2 is added to the nanocomposite samples, which raises the levels of hydroxyl groups and speeds up the vulcanization process. As a result, the hydroxyl group increased the crosslinking reaction. Overall, nanocomposites cured by MBTS showed a more rapid cure rate than the CBS system. It is shown by the CRI index of more than 200 observed for the compounds. An analysis of the CRI values revealed that increasing the loading of tin dioxide (SnO_2) filler significantly enhanced the curing efficiency. This resulted in a shorter duration for the compound to cure once it reached the scorch time. The fast curing exhibited by the MBTS accelerator system directly results from the system facilitated by thiazole groups, which is more efficient than the sulphonamides groups in the CBS system [25]. When examining the flow characteristics of the compounds under heat, a decreasing pattern was observed for ML, MH and MH-ML with SnO_2 loadings. This indicates the ability of SnO_2 to function as a plasticizer. The flowability of the melt was improved in the nanocomposite compounds cured by the CBS system. The viscosity represented by the ML values ranged between 0.3 to 0.5 dNm for the CBS-cured nanocomposites.

In contrast, the ML values for MBTS-cured systems were between 8.6 to 13.2 dNm. These observations align well with the findings reported by Indrajati and Dewi [26], which state that MBTS-based systems exhibit a higher Mooney viscosity than CBS-based systems at the same concentration. High Mooney viscosity is associated with the early dominance of elastic elements during curing [26]. Therefore, SnO_2 is crucial in delaying curing and reducing melt viscosity. This effect is consistent for both compounds, regardless of the accelerator systems used.

Therefore, the nanocomposite compounds cured by the CBS system are suitable for safer and easier processability. Hence, the following tests and analyses were only performed on the DPNR nanocomposites formulated with the CBS system.

3.2 Swell Measurement

Figure 2 shows the swelling behaviour of DPNR composites under the toluene immersion test. The swelling test of the DPNR nanocomposites was performed in the toluene solutions for 72 hours and the values were taken for 24 hours, 48 hours and 72 hours.

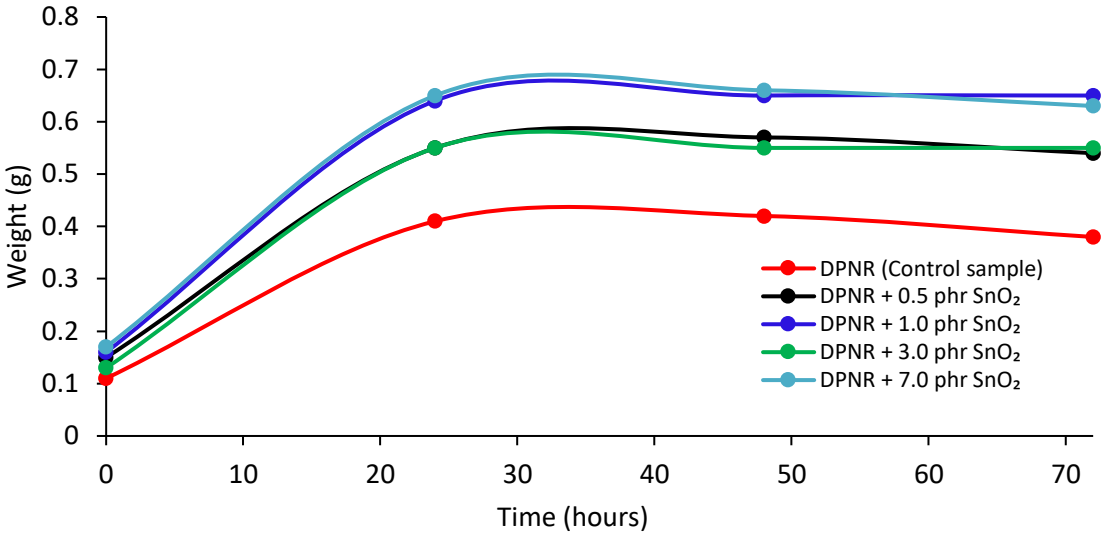

Fig. 2. Swelling measurement of DPNR reinforced by SnO_2 filler loadings

The swelling test was used to assess the solvent resistance behaviour of the DPNR nanocomposites produced. Figure 2 depicts the weight changes of the composites filled with varying amounts of SnO_2 particles over time. The amount of toluene uptake increased steadily over time until it reached the saturation limit in about 24 hours. The swelling percentages showed constant values from 24 hours up to 72 hours. A slight drop was observed for the control sample after reaching 48 hours. It reflected the shrinkage experienced by the samples. Meanwhile, with the presence of the SnO_2 particles, the swell percentages were more consistent even after 72 hours.

3.3 Density

Table 3 depicts the density of DPNR composites at different filler loadings. The density showed an increment pattern as the filler loading increased. Increasing the SnO_2 particles in the rubber matrix would theoretically cause the density to increase because of the contributions of the high-density SnO_2 powders compared to the density of the DPNR.

Table 3
Density and hardness of DPNR reinforced by SnO_2 nanocomposites at various filler loadings

Samples	CBS system	
	Density (g/cm^3)	Hardness (Shore A)
DPNR	0.910 ± 0.042	38.02 ± 0.44
DPNR + 0.5 phr SnO_2	0.911 ± 0.036	34.96 ± 0.59
DPNR + 1.0 phr SnO_2	0.936 ± 0.014	35.58 ± 0.25
DPNR + 3.0 phr SnO_2	0.950 ± 0.008	35.56 ± 0.44
DPNR + 7.0 phr SnO_2	1.041 ± 0.014	35.98 ± 0.33

3.4 Hardness

Table 3 shows the hardness values for the DPNR reinforced by SnO_2 nanoparticles for the effect of filler loadings. The hardness properties agree with the results obtained from the MH values. The reduction in hardness is related to the decrease in MH values obtained by the composites due to the chain softening by the SnO_2 particles. Regardless of adding high hardness and high modulus SnO_2 nanoparticles, the capability of the particles to ease the chain movement under deformation reduced the stress to deform the material under localized force. A typical elastomer compound's main constituents are long-chain molecules known as the base polymer, which provide the basic chemical and physical properties. A small amount of free space exists between the long chain molecules, allowing the elastomeric molecules to deform and change shapes independently of one another [17]. Hence, lower indentation energy was required to deform the surface of the DPNR composites with SnO_2 filler particles compared to the control sample.

3.5 Thermal Characteristics using Dynamic Mechanical Thermal Analyzer (DMTA)

Figure 3 shows the thermal analysis results of DPNR and DPNR composites. The storage modulus (E') is a parameter that quantifies the energy stored and subsequently recovered in each deformation cycle. Essentially, it serves as an indicator of a material's stiffness. A higher storage modulus corresponds to a stiffer material, which resists deformation more effectively. On the other hand, the loss modulus (E") measures the energy dissipated during a deformation cycle, typically heat. This parameter is crucial in understanding how a material behaves under cyclic loading conditions, as it provides insights into the energy loss that occurs due to internal friction. The ratio of the loss modulus to the storage modulus is defined as Tan δ. This value is particularly significant in studying polymeric materials, representing their damping properties. Damping refers to the ability of a material to dissipate energy and a higher Tan δ value indicates greater damping.

In this study, the addition of tin dioxide had a noticeable impact on these properties. Incorporating SnO_2 filler particles reduced the chain's stiffness and the energy lost due to hysteresis. This observation aligns well with the observed decrease in MH and hardness values, suggesting a consistent effect of tin dioxide addition on these material properties. Interestingly, the Tan δ value exhibited a non-linear response to tin dioxide loading. It increased when the loading of tin dioxide was at 3.0 phr but decreased when it reached 7.0 phr. This suggests that an overloading of tin dioxide can diminish the reinforcing effect of the nanoparticle fillers on the DPNR matrix. This could be due to the agglomeration of nanoparticles at higher loadings [27], which can disrupt the dispersion of fillers and consequently reduce their reinforcing effect.

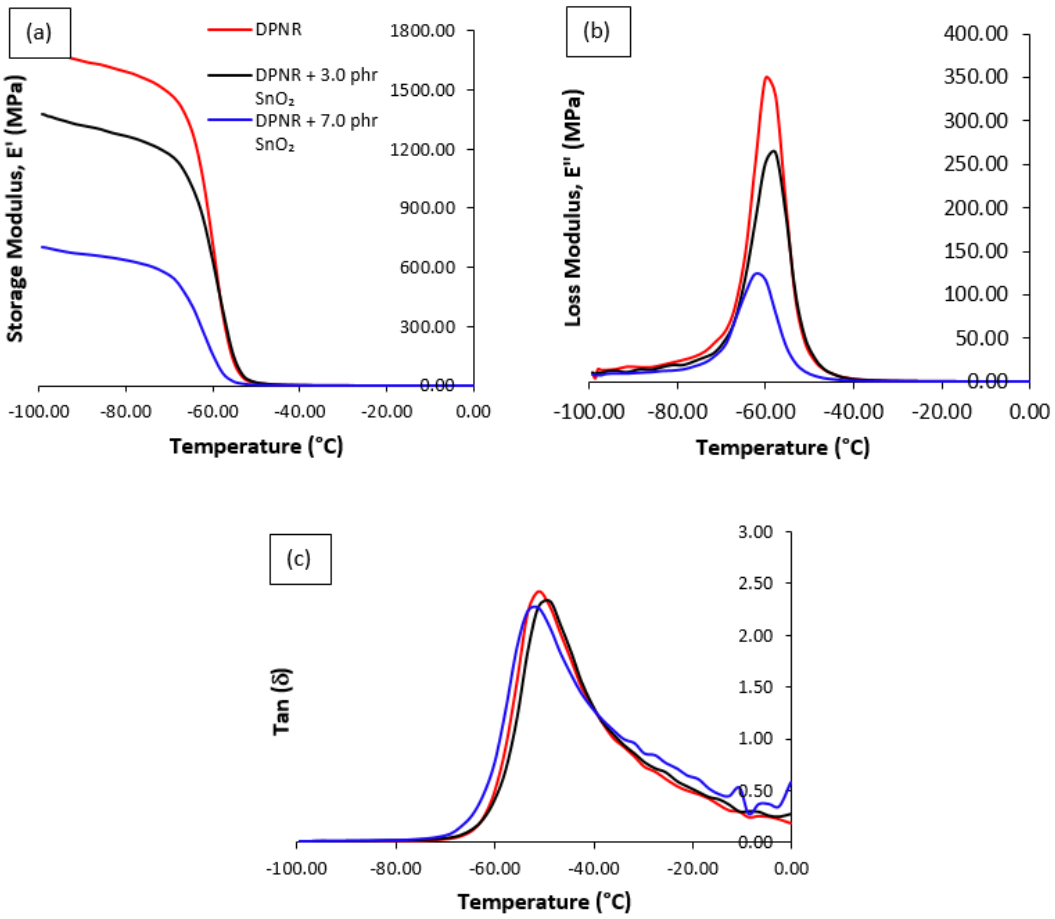

Fig. 3. DMTA analysis of (a) storage modulus (b) loss modulus (c) tan delta of DPNR, DPNR with 3.0 phr SnO_2 and DPNR with 7.0 phr SnO_2

3.6 Morphological and Topology Characteristics by SEM and AFM

Figure 4 shows SEM micrographs of tensile fracture surfaces at magnifications of 200X and 2000X for DPNR reinforced by 0, 3.0 and 7.0 phr SnO_2. The continuous phase indicated the DPNR matrix; meanwhile, the discrete phases were combinations of dispersed SnO_2, ZnO and sulphur particles. From the micrographs, dispersed particles are uniformly distributed throughout the matrix, especially observed in the composite reinforced by the 3.0 phr SnO_2. The discrete particles distributed uniformly throughout the matrix indicate consistent properties of the composites. Therefore, it is clear that the composites were successfully produced using the selected curing system. Several energy absorption mechanisms were present from the fractured surfaces, such as matrix yielding from matrix phase debonding and filler pull-out. The degree of plastic deformation experienced by the composites indicates the extent of stresses endured by the samples before failure. All of the micrographs exhibit ductile failure with obvious traces of tearing and matrix yielding. But, the composite at 3.0 phr SnO_2 showed a more ductile failure. It showed rougher surfaces with thinner yielded lines from the deformation. This observation is in line with the decrease of MH, indicating higher flexibility of the composite at this level.

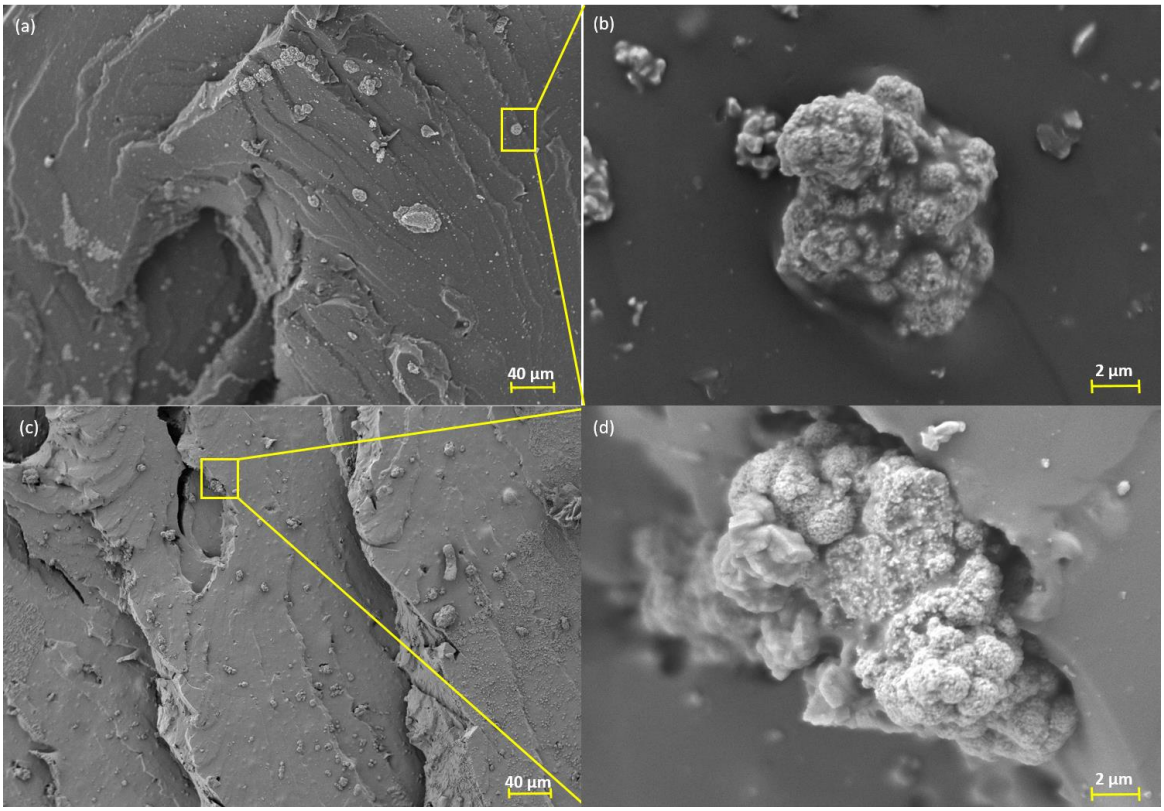

Fig. 4. SEM images of fractured surfaces of DPNR reinforced SnO2 at 3.0 phr at (a) 200X and (b) 2000X magnifications and 7.0 phr at (c) 200X and (d) 2000X magnifications

Meanwhile, the fracture mode appeared more brittle at a SnO_2 level of 7.0 phr. It showed a lesser plastic-yielding mechanism and a smoother surface. This might be the direct effect of a worsened dispersion level at a loading of SnO_2 particles that is too high. There were clusters with sizes larger than their original particles [27], forming agglomerates of about 20 µm. These agglomerates would have become the stress concentrators and initiated cracks in the composites. Obvious cracks are observed for both DPNR without SnO_2 and DPNR reinforced by 7.0 phr SnO_2 particles. Atomic Force Microscopy (AFM) was employed to analyse the morphology and topology of the samples, as illustrated in Figure 5. This analysis revealed a correlation between the surface roughness and the filler content; an increase in filler content led to a corresponding increase in surface roughness.

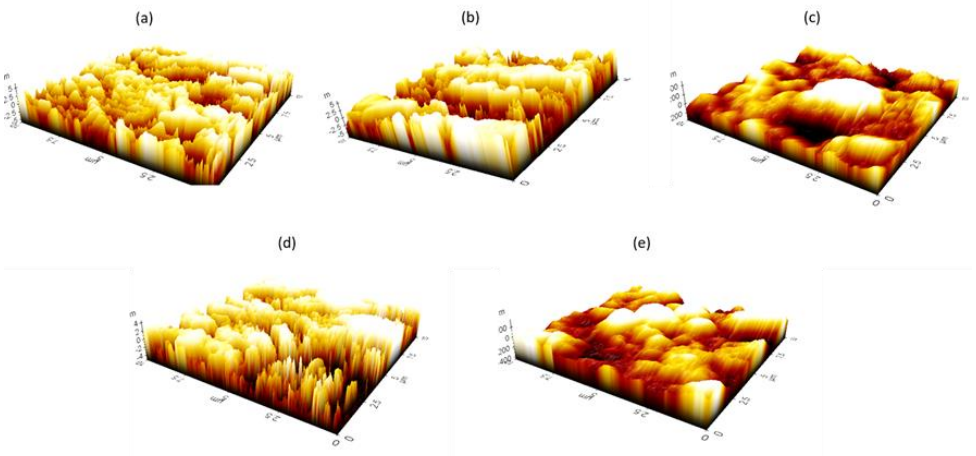

Fig. 5. AFM topography analysis of (a) DPNR and DPNR reinforced with SnO_2 at (b) 0.5 phr (c) 1.0 phr (d) 3.0 phr (e) 7.0 phr

In the samples containing fillers, the lighter regions predominantly represent the peaks of the fillers on the fractured surfaces. Conversely, the darker regions correspond to the depths of the asperities, represented as negative values from the zero level. The most profound depths, reaching up to -400 nm, were primarily observed in the samples reinforced with the highest concentration of SnO_2 nanoparticles. The darker regions surrounding the remaining pull-out mechanisms were typically present in these samples. Interestingly, in the sample containing 3.0 phr nanoparticles, the darker regions provided evidence of plastic deformation due to the applied force, indicating a higher degree of ductile fracture. This suggests that the filler content influences the surface roughness and affects the material's mechanical properties.

3.7 Compositional Characteristics FTIR

Figure 6 depicts the IR spectra of pristine DPNR with comparisons with DPNR reinforced by SnO_2 filler at 3.0 and 7.0 phr. Only these two samples were selected to compare compositional characteristics between the best (3.0 phr) and worst samples (7.0 phr) against the control sample. Overall, there are obvious differences between DPNR with and without the SnO_2 particles. The peaks are located between 2000 and 2500 cm^{-1} and 3500 and 4000 cm^{-1}. Therefore, the newly dictated peaks were associated with SnO_2 filler loadings in DPNR.

The IR spectra support the results of the cure characteristics since the functional groups on the uncalcined SnO_2 nanoparticles changed the DPNR matrix's molecular makeup. The 550-650 cm^{-1} bands were ascribed to Sn-O-Sn and Sn-OH stretching modes. On uncalcined SnO_2 surfaces, significant bands at 2922, 2841 and 1400 cm^{-1} were attributed to C-H stretching and bending vibrations [28]. Meanwhile, the 3500 to 4000 cm^{-1} peaks indicate the presence of hydroxyl groups in the composites [29,30]. The groups were present on the uncalcined SnO_2 before the compounding process.

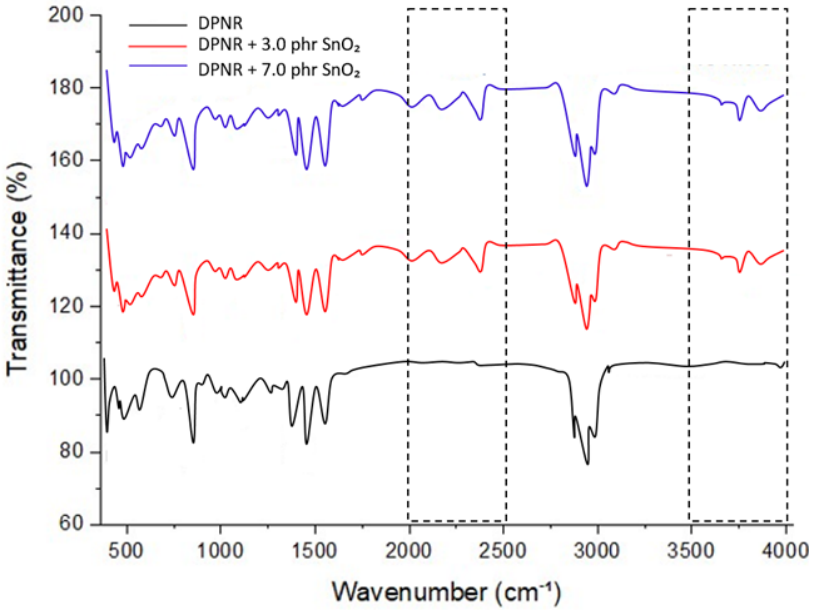

Fig. 6. FTIR Spectra of DPNR, DPNR with 1.0 phr SnO_2 and DPNR with 7.0 phr SnO_2

4. Conclusions

The curing characteristics, density and hardness of the DPNR nanocomposites were examined as a function of different accelerator systems and SnO_2 nanoparticle loading. The CBS-cured nanocomposites had higher process safety and good melt flow for processing than the MBTS-cured system. The contributions of SnO_2 in both compounds were similar and it is shown to act as a plasticizer and curing retarder in the SnO_2-reinforced DPNR nanocomposites. The density and hardness of the DPNR composites agreed with the changes in torque values of the DPNR compounds for the various SnO_2 loadings. The softer DPNR nanocomposites manifested morphology for a more ductile failure under stress deformation. The addition of uncalcined SnO_2 showed evidence of compositional changes, which altered the cure characteristics due to the presence of active functional groups.

Acknowledgement

The authors would like to thank the Tin Industry (Research and Development) Board, Kementerian Air, Tanah Dan Sumber Asli, Malaysia, for the KHAS-TIN/2021/FKP/C00007 grant and Universiti Teknikal Malaysia Melaka (UTeM) and Rubber Leisure Products Sdn. Bhd. for facilities and supports.

References

[1] Wang, Peng, Qizhi Chen, Jiaxuan Zhang and Zinan Wang. "Research on the Influence of Nanoparticles and Surface Microstructure on the Hydrophobic and Electrical Properties of Silicone Rubber Materials." In *Electrical Materials: Performance Improvement, Recent Advances and Engineering Applications*, pp. 189-216. Singapore: Springer Nature Singapore, 2024. https://doi.org/10.1007/978-981-99-9050-4_5

[2] Zuidema, Carl, Wes Kegerise, Robert Fleming, Mark Welker and Steven Boggs. "A short history of rubber cables." *IEEE Electrical Insulation Magazine* 27, no. 4 (2011): 45-50. https://doi.org/10.1109/MEI.2011.5954068

[3] Junian, S., M. Z. H. Makmud and J. Sahari. "Natural rubber as electrical insulator: A review." *J. Adv. Rev. Sci. Res* 6 (2015): 28-42.

[4] Anggaravidya, Mahendra, Akhmad Amry, Dewi K. Arti, Eryanti Kalembang, Herri Susanto, Ade S. Hidayat and Caroline D. Limansubroto. "Properties of natural rubber/chloroprene rubber blend for rubber fender application: Effects of blend ratio." In *Macromolecular Symposia*, vol. 391, no. 1, p. 1900150. 2020. https://doi.org/10.1002/masy.201900150

[5] Panklang, Nitipong, Nathabhat Phankong and Krischonme Bhumkittipich. "Design of 33 kV Transformer Bushing Insulator from NR and HDPE." *Energy Procedia* 9 (2011): 95-103. https://doi.org/10.1016/j.egypro.2011.09.011

[6] Thumwong, Arkarapol, Worawat Poltabtim, Patcharaporn Kerdsang and Kiadtisak Saenboonruang. "Roles of Chitosan as bio-fillers in radiation-vulcanized natural rubber latex and hybrid radiation and peroxide-vulcanized natural rubber latex: Physical/mechanical properties under thermal aging and biodegradability." *Polymers* 13, no. 22 (2021): 3940. https://doi.org/10.3390/polym13223940

[7] Pichaiyut, Skulrat, Chalermphong Uttaro, Kritnarong Ritthikan and Charoen Nakason. "Biodegradable thermoplastic natural rubber based on natural rubber and thermoplastic starch blends." *Journal of Polymer Research* 30, no. 1 (2023): 23. https://doi.org/10.1007/s10965-022-03406-7

[8] Puad, Farah Hamizah, Nawrah Afnan Ashraf and Fadzidah Mohd Idris. "Fabrication and Characterization of Nanocoils CNT/PLA Filament at Different Filler's Percentages as Electromagnetic Wave Absorbers." *Journal of Advanced Research in Micro and Nano Engineering* 19, no. 1 (2024): 86-98. https://doi.org/10.37934/armne.19.1.8698

[9] Mohamad, Noraiham, Hairul Effendy Ab Maulod, Jeefferie Abd Razak, Mohd Sharin Ghani, Nor Hidayah Rahim, Mohd Hanafiah Mohd Isa, Dewi Suriyani Che Halin, Mohammed Iqbal Shueb and Norshafarina Ismail. "Tensile and Dielectric Properties of Tin Dioxide Reinforced Deproteinized Natural Rubber Nanocomposites for Electrical Insulator." In *Green Materials and Electronic Packaging Interconnect Technology Symposium*, pp. 221-229. Singapore: Springer Nature Singapore, 2022. https://doi.org/10.1007/978-981-19-9267-4_26

[10] Zulfiqar, Rajwali Khan, Yuliang Yuan, Zainab Iqbal, Jie Yang, Weicheng Wang, Zhizhen Ye and Jianguo Lu. "Variation of structural, optical, dielectric and magnetic properties of SnO 2 nanoparticles." *Journal of Materials Science: Materials in Electronics* 28 (2017): 4625-4636. https://doi.org/10.1007/s10854-016-6101-1

[11] Kolmakov, A., D. O. Klenov, Y. Lilach, S. Stemmer and M. Moskovits. "Enhanced gas sensing by individual SnO2 nanowires and nanobelts functionalized with Pd catalyst particles." *Nano letters* 5, no. 4 (2005): 667-673. https://doi.org/10.1021/nl050082v
[12] Rahim, N. H., K. Y. Lau, N. A. Muhamad, N. Mohamad, W. A. W. A. Rahman and A. S. Vaughan. "Effects of filler calcination on structure and dielectric properties of polyethylene/silica nanocomposites." *IEEE Transactions on Dielectrics and Electrical Insulation* 26, no. 1 (2019): 284-291. https://doi.org/10.1109/TDEI.2018.007796
[13] Zhuravlev, L. T. "The surface chemistry of amorphous silica. Zhuravlev model." *Colloids and Surfaces A: Physicochemical and Engineering Aspects* 173, no. 1-3 (2000): 1-38. https://doi.org/10.1016/S0927-7757(00)00556-2
[14] Alimin, Mahyudin, Arief Syukri and Abral Hairul. "Mechanical Properties and Biodegradability of Areca Nut Fiber-reinforced Polymer Blend Composites." *Evergreen* 7, no. 3 (2020): 366-372. https://doi.org/10.5109/4068618
[15] Honorato, Luciana Ribeiro, Leila Lea Yuan Visconte and Regina Célia Reis Nunes. "Effect of different cure systems on natural rubber/nanocellulose nanocomposites in rheological, physical-mechanical, aging and mechanical properties." *Journal of Elastomers & Plastics* 54, no. 5 (2022): 676-692. https://doi.org/10.1177/00952443221077438
[16] Hong, Choy Jun, Noraiham Mohamad, Hairul Effendy Ab Maulod, Jeefferie Abd Razak, Toibah Abd Rahim, Mohd Sharin Ghani, Nor Hidayah Rahim, Soh Tiak Chuan, Dewi Suriyani Che Halin and Mohammed Iqbal Shueb. "Crosslink Density and Toluene Sorption of Tin Dioxide Reinforced Deproteinized Natural Rubber Nanocomposites." *Journal of Advanced Research in Applied Mechanics* 111, no. 1 (2023): 103-119.
[17] Mohamad, N., J. Yaakub, H. E. Ab Maulod, A. R. Jeefferie, M. Y. Yuhazri, K. T. Lau, Q. Ahsan, M. I. Shueb and R. Othman. "Vibrational damping behaviors of graphene nanoplatelets reinforced NR/EPDM nanocomposites." *Journal of Mechanical Engineering and Sciences* 11, no. 4 (2017): 3274-3287.
[18] Ghorai, Soumyajit, Arun Kumar Jalan, Madhusudan Roy, Amit Das and Debapriya De. "Tuning of accelerator and curing system in devulcanized green natural rubber compounds." *Polymer testing* 69 (2018): 133-145. https://doi.org/10.1016/j.polymertesting.2018.05.015
[19] Hayeemasae, Nabil and Hanafi Ismail. "Optimization of Accelerators on the Properties of Natural Rubber/Recycled Ethylene Propylene Diene Rubber Blends." In *Recycled Polymer Blends and Composites: Processing, Properties and Applications*, pp. 209-226. Cham: Springer International Publishing, 2023. https://doi.org/10.1007/978-3-031-37046-5_10
[20] Ghorai, Soumyajit, Dipankar Mondal, Sakrit Hait, Anik Kumar Ghosh, Sven Wiessner, Amit Das and Debapriya De. "Devulcanization of waste rubber and generation of active sites for silica reinforcement." *ACS omega* 4, no. 18 (2019): 17623-17633. https://doi.org/10.1021/acsomega.9b01424
[21] Kaliyathan, Abitha Vayyaprontavida, Ajay Vasudeo Rane, Stefan Jackson and Sabu Thomas. "Analysis of diffusion characteristics for aromatic solvents through carbon black filled natural rubber/butadiene rubber blends." *Polymer Composites* 42, no. 1 (2021): 375-396. https://doi.org/10.1002/pc.25832
[22] Yotkuna, Khrongkhwan, Rungsima Chollakup, Tanawat Imboon, Venkatramanan Kannan and Sirikanjana Thongmee. "Effect of flame retardant on the physical and mechanical properties of natural rubber and sugarcane bagasse composites." *Journal of Polymer Research* 28 (2021): 1-13. https://doi.org/10.1007/s10965-021-02805-6
[23] Nor, NA Mohd and N. Othman. "Effect of filler loading on curing characteristic and tensile properties of palygorskite natural rubber nanocomposites." *Procedia Chemistry* 19 (2016): 351-358. https://doi.org/10.1016/j.proche.2016.03.023
[24] Chang, Young-Wook, Yungchul Yang, Seunghoon Ryu and Changwoon Nah. "Preparation and properties of EPDM/organomontmorillonite hybrid nanocomposites." *Polymer International* 51, no. 4 (2002): 319-324. https://doi.org/10.1002/pi.831
[25] Maciejewska, Magdalena and Monika Siwek. "The influence of curing systems on the cure characteristics and physical properties of styrene–butadiene elastomer." *Materials* 13, no. 23 (2020): 5329. https://doi.org/10.3390/ma13235329
[26] Indrajati, Ihda Novia and Indiah Ratna Dewi. "Performance of binary accelarator system on natural rubber compound." *Majalah Kulit, Karet, dan Plastik* 34, no. 2 (2019): 49-60. https://doi.org/10.20543/mkkp.v34i2.4049
[27] Sethulekshmi, A. S., Appukuttan Saritha and Kuruvilla Joseph. "A comprehensive review on the recent advancements in natural rubber nanocomposites." *International Journal of Biological Macromolecules* 194 (2022): 819-842. https://doi.org/10.1016/j.ijbiomac.2021.11.134
[28] Farrukh, Muhammad Akhyar, Heng Boon Teck and Rohana Adnan. "Surfactant-controlled aqueous synthesis of SnO_2 nanoparticles via the hydrothermal and conventional heating methods." *Turkish Journal of Chemistry* 34, no. 4 (2010): 537-550. https://doi.org/10.3906/kim-1001-466

[29] Supramaniam, Janarthanan, Darren Yi Sern Low, See Kiat Wong, Bey Fen Leo, Bey Hing Goh and Siah Ying Tang. "Nano-engineered ZnO/CNF-based epoxidized natural rubber with enhanced strength for novel Self-healing glove fabrication." *Chemical Engineering Journal* 437 (2022): 135440. https://doi.org/10.1016/j.cej.2022.135440

[30] Ellerbrock, Ruth, Mathias Stein and Jörg Schaller. "Comparing amorphous silica, short-range-ordered silicates and silicic acid species by FTIR." *Scientific Reports* 12, no. 1 (2022): 11708. https://doi.org/10.1038/s41598-022-15882-4